Statistics of avalanches in martensitic transformations. I. Acoustic emission experiments

Eduard Vives, Ismael Ràfols, Lluís Mañosa, Jordi Ortín, and Antoni Planes
Departament d'Estructura i Constituents de la Matèria, Facultat de Física, Universitat de Barcelona, Diagonal 647, E-08028 Barcelona, Catalonia, Spain
(Received 16 May 1995)

We present an experimental study of the transformation avalanches taking place during a thermally induced thermoelastic martensitic phase transition of a Cu-Zn-Al alloy. We have studied the statistical distribution of amplitudes and durations of the acoustic emission signals released in the avalanches and found them to exhibit power-law behavior in more than one decade. Distributions measured around different temperatures along the transformation path are found to be equivalent. We have measured the exponents for the distribution of amplitudes ($\alpha = 3.6 \pm 0.8$) and durations ($\tau = 3.5 \pm 0.8$), for the statistical dependence of amplitudes on durations ($x = 1.0 \pm 0.1$) and for the power spectrum of trains of measured acoustic signals ($\phi = 0.9 \pm 0.1$).

I. INTRODUCTION

A martensitic transformation is a structural, first-order and diffusionless phase transition. The discontinuous change in symmetry and shape of the unit cell is mainly described by a combination of shears in specially favorable directions. On cooling, the transition starts at a given temperature M_s by the nucleation of product phase. This is accompanied by the development of long-range strain fields in the parent lattice, arising from the difference in shape between the unit cells of parent and product phases. The observed typical arrangements of polydomain structures are such that minimize the stored elastic energy.[1] When a small fraction of the product phase exists, the effect of the resulting stored elastic energy is to block the transformation, and subsequent increase in the amount of product phase needs additional undercooling. As a consequence, the transition takes place in a broad range of temperatures between M_s and the temperature M_f for which the full system is transformed. The transformation path follows a succession of metastable two phase states. Thermal fluctuations appear to be irrelevant for this class of transitions. The role of temperature is to determine the free-energy difference between the two phases, providing the driving force for the transition. On heating the reverse transition occurs with hysteresis, starting at $A_s > M_f$ and finishing at $A_f > M_s$.

The relaxation from one metastable state to another metastable state takes place through avalanches with an associated energy dissipation, responsible for the hysteresis observed in these transitions. The origin of the avalanches may be due to either simultaneous motions of interfaces located in different (spatially correlated or not) places of the crystal, or to the discontinuous motion of a single interface. At each avalanche, in addition to the latent heat associated to the fraction of transformed material, elastic energy is irreversibly released in the form of elastic waves. The waves are emitted in the ultrasonic range and are known as acoustic emission (AE).[2] Actually there is little information on the AE source and on the specific origin of the avalanches.[3]

A study of the statistical distribution of amplitudes A and durations T of the AE signals associated with the avalanches has recently been reported.[4] The important result to be stressed is that both quantities exhibit power-law distributions. This is an indication that the system evolves without characteristic time and length scales, which is a typical feature of criticality. The open question is the origin of such criticality. An answer has recently been given by Sethna *et al.* in a set of recent papers,[5] in which they suggest that the intrinsic disorder in the system is responsible for such behavior. These authors propose a model exhibiting a fluctuationless first-order phase transition, consisting in a random-field Ising model at zero temperature with an applied external field. By changing the external field the transition takes place through avalanches, whose size distribution depends on the amount of disorder in the system. For a small degree of disorder the system exhibits an infinite avalanche, while for a large degree of disorder the avalanches are very tiny and the transition extends in a broad range of the external applied field. An important point is that for a critical value of the disorder the distribution of avalanches is power law. A similar behavior has been obtained in the random bond Ising model[6] and in the three-states Blume-Emery-Griffiths model[7] with disorder.

In real martensitic systems the disorder has two principal origins: (i) static disorder associated with quenched-in defects such as vacancies, interstitials, impurities, dislocations, off-stoichiometry and (ii) disorder of a dynamic nature arising from competing long-range (elastic) interactions between domains. An important difference between martensitic systems and models comes from the fact that martensites exhibit disorder that is not quenched but modified by the domain evolution: permanent defects are created and the field of internal stresses is modified. This fact, to our knowledge, has never been theoretically considered.

The aim of this work is to characterize the critical state in the case of a Cu-Zn-Al alloy undergoing a martensitic transformation. For clarity, we have divided the work in two parts. Here, in part I, we provide details of acoustic emission experiments, histograms of amplitudes and durations, the correlation function of the measured signals, and the exponents characterizing the distributions. Such results complete

0163-1829/95/52(17)/12644(7)/$06.00

and occasionally correct those presented in a previous letter.[4] In part II we provide a general model, based on scaling arguments, for the description of the joint distribution of any pair of magnitudes characterizing spatial and temporal scales of avalanches. In particular the model is applied to the data presented in this first part.

II. EXPERIMENTAL

A. Experimental setup

A single crystal grown by the Bridgman method from elements of purity 99.99%, with composition Cu-17.0% Zn-13.7 at. % Al, has been investigated. A disk-shaped specimen of 12.6 mm diameter and 1.9 mm thickness has been cut from the original crystal using a low speed diamond saw and the surfaces have been mechanically polished. On cooling the transition starts at $M_s \approx 299$ K and finishes at $M_f \approx 268$ K. The transition temperatures of the reverse transformation, on heating, are $A_s \approx 278$ K and $A_f \approx 308$ K. We have performed several hundreds of heating and cooling cycles between 260 and 330 K in order to ensure a very good reproducibility of the hysteresis cycle.

The sample is placed on the surface of a copper block which is heated or cooled by means of a thermoelectric battery using the Peltier effect. The high thermal conductivity of both sample and copper block ensures that the temperature is essentially homogeneous and therefore the temperature of the sample can be taken to be the same as the temperature of the copper block. The temperature of the block is controlled by a PC computer in the following way: the temperature is measured with a four wire Pt-100 resistance probe, using an HP-34401A multimeter; the reading is sent to the computer, and compared against the programmed temperature. Based on the comparison the computer instructs an HP-59501B digital-to-analog converter to command an Electronic Measurements BOS/S 20-5 power supply to drive the thermoelectric battery. A simple feedback algorithm allows control of both the temperature and its temporal derivative with accuracies better than 0.3 K and 0.01 K/min, respectively, for heating and cooling rates ranging from 0.1 to 8 K/min.

AE signals are detected by a resonant piezoelectric transducer (axial resonance frequency: ~ 2 MHz), acoustically coupled to the surface of the sample by a thin layer of silicon oil. The electric signal from the transducer is amplified and filtered in the frequency range 400 kHz–2 MHz by a Bruel and Kjaer preamplifier and amplifier. The overall amplification used in the experiments is 60 dB. The dc output of the amplifier has been modified to provide a peak with an amplitude equal to the positive level of the signal, a short rise time (0.2 μs) and a decay time constant of 16 μs. This peak is recorded using a fast transient digitizing HP-59501B oscilloscope at a sampling frequency of 0.5 MHz. The background noise is found to be mainly of electric nature. The noise of mechanical nature has a frequency typically much lower than the studied range, and a possible source of noise, due to temperature fluctuations inducing the inverse transition, is not present since the transition exhibits hysteresis.

We have followed two different procedures in the acquisition of signals:

(1) A first set of experiments is performed by acquisition of blocks of 1000 consecutive signals with amplitudes higher than a trigger level of 4×10^{-4} V. The background noise is 1×10^{-4} V. The maximum amplitude A and duration T of each signal are measured (see Fig. 1). Despite the trigger level, amplitudes below 4×10^{-4} V have been apparently detected due to the fact that the trigger is analog, while the amplitude measurements are sampled in time. The duration is calculated using the upper-mid-lower threshold algorithm[8] provided by the oscilloscope. These measurements are performed in small temperature intervals (~ 0.5 K) centered at different temperatures (268, 273, 278, 283, and 288 K during cooling and 283, 288, 293, 298, and 303 K during heating). The total number of measured signals is about 2×10^4. We have verified that the results are independent of the cooling and heating rates in the range from 0.1 to 8 K/min. The available ranges of A and T are limited by the following experimental window:

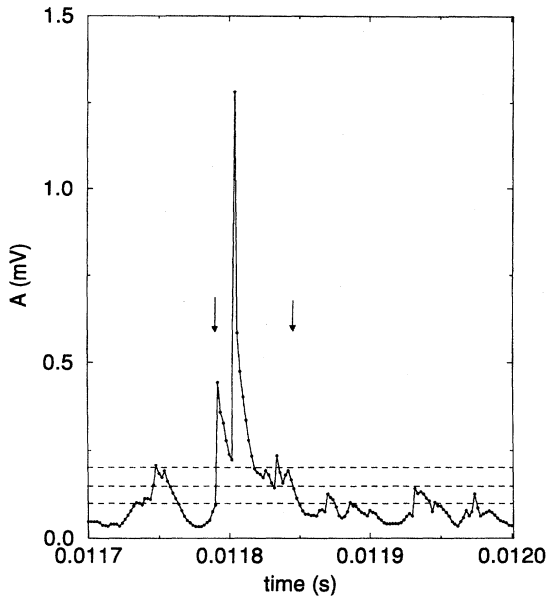

FIG. 1. Example of a typical digitized AE signal. The dashed lines show the low, mid, and upper threshold used for the determination of the duration of a signal.

(a) *Low amplitude limit.* The trigger-level $A_{\min} = 4\times10^{-4}$ V. Any smaller signal is discarded in the subsequent analysis.

(b) *High amplitude limit.* The oscilloscope maximum range is set at 8×10^{-3} V. Nevertheless, the lack of statistics does not allow to observe any signal with amplitude higher than 5×10^{-3} V. Therefore we consider $A_{\max} = 5\times10^{-3}$ V.

(c) *Low duration limit.* Data are sampled at 0.2 μs. Nevertheless, due to the existence of high-frequency electric noise, a value $T_{\min} = 10^{-5}$ s is taken, and signals shorter than this value are discarded for the analysis.

(d) *High duration limit.* The oscilloscope scale is set to 7×10^{-4} s. Nevertheless, the lack of statistics does not allow to observe any signal longer than $T_{max}=5\times10^{-4}$ s.
Such experimental window reduces the number of analyzed signals to ~8000 for cooling and ~8500 for heating.

(2) A second set of experiments consists in the acquisition of long (16 ms) sequences of AE signals, $\Psi(t)$, aimed to calculate the time correlation function and the power spectrum. Two sets of 20 sequences have been measured at 283 K for cooling and 293 K for heating. The same experimental limits apply for this case although, since the statistics is poorer, no signals with $T>5\times10^{-5}$ s have been recorded.

B. Calibration

To calibrate the chain formed by the amplifier and the oscilloscope we have simulated the AE signals by generating a sequence of sinusoidal pulses (250 kHz) separated 1 ms, with amplitudes ranging between 20 and 800 mV and durations ranging from 10 to 600 μs using an HP3314A pulse generator. The following two calibration equations have been obtained:

$$A=\frac{A_m}{1.2}\ , \tag{1}$$

$$T=T_m-(13.0\ \mu\text{s})\ln\frac{A_m}{0.18\ \text{mV}}\ , \tag{2}$$

where A_m and T_m are the measured values for an input signal with amplitude A and duration T. The correction to the amplitude is due to the fact that, since we are measuring the maximum value, the noise always gives a positive contribution. This factor depends negligibly on A and T. The correction to the measured duration is due to the time constant of the amplifier which has been set to 16 μs.

III. RESULTS

A. Joint and marginal histograms

Figure 2 shows a three-dimensional plot and the map of the joint histograms of A and T corresponding to all the recorded signals during cooling and heating. A and T axis are logarithmic while the vertical axis shows the number of signals in linear scale. The histogram has been obtained using a logarithmic mesh of 20×20 ranging from 10^{-4} to 10^{-2} V and from 10^{-6} to 10^{-3} s. The contour levels in the map are spaced 100 counts starting from 100. The small peak below 5×10^{-6} s is due to electric noise, inherent to the experimental system. A tendency for the data to distribute along a line ($A\sim T^x$) can be clearly observed.

Figures 3 and 4 show log-log plots of the histograms of signals with amplitude A and duration T, respectively. Data corresponding to heating and cooling transformations are plotted with different symbols. Arrows indicate the position

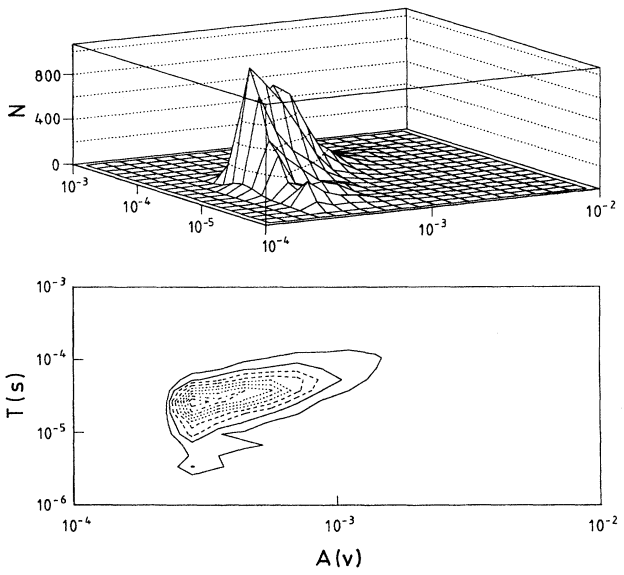

FIG. 2. (Top) $3d$ plot of the joint histogram of AE signals $p(A,T)$ for cooling and heating data. The histogram has been calculated using a logarithmic 20×20 grid ranging from 10^{-4} to 10^{-2} V in amplitude and from 10^{-6} to 10^{-3} s in duration. (Bottom) The map of the above $3d$ plot showing contour levels spaced 100 counts starting from 100 counts.

of the experimental window limits, within which data are reliable. The vertical axis corresponds to the number of counts p normalized within the experimental limits. It is apparent from the figures that these histograms conform to power-law distributions of the form $A^{-\alpha}$ and $T^{-\tau}$. The bend observed in $p(T)$ is due to the cutoff in the amplitudes which distorts the statistics of durations below 8×10^{-5} s. This

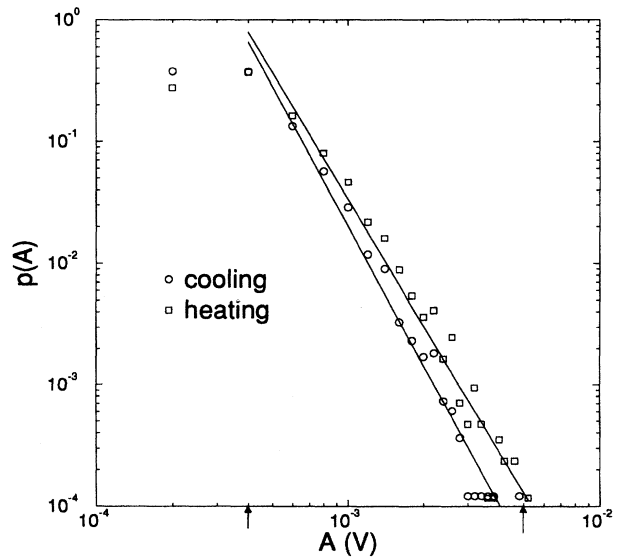

FIG. 3. $p(A)$ for cooling (circles) and heating (squares), together with least-squares fits with slopes $\alpha=3.8$ and $\alpha=3.5$, respectively. Arrows indicate the experimental limits within which data are reliable.

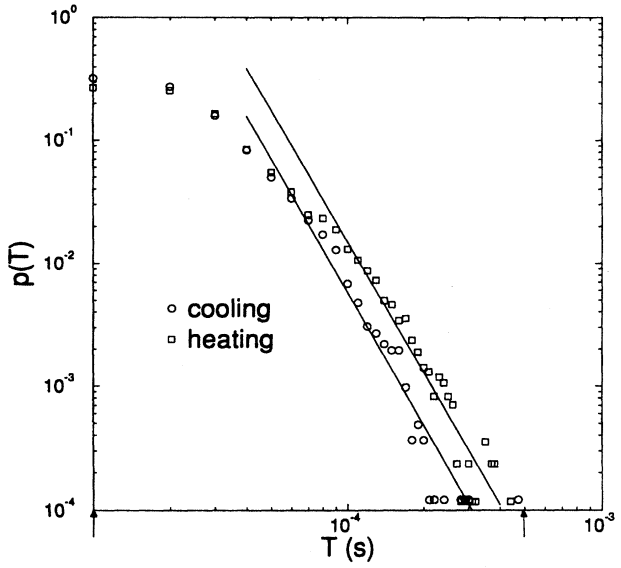

FIG. 4. $p(T)$ for cooling (circles) and heating (squares), together with least-squares fits with slopes $\tau=3.6$ and $\tau=3.5$, respectively. Arrows indicate the experimental limits within which data are reliable.

window effect was not taken into account in a first set of experiments reported previously.[4] We will discuss its implications in detail in a subsequent paper (part II).

B. Temperature dependence

Figures 5 and 6 show the histograms for A and T obtained in acquisitions centered at different temperatures during forward and reverse transformations. Within the experimental uncertainties, the histograms show that the corresponding distributions are independent of temperature, indicating that the physical behavior of the system is the same all along the transformation, i.e., the first domains to transform behave statistically in the same way as the last ones. An interesting remark concerns the histograms for amplitudes and durations in the forward transformation. It can be seen that the breakdown of the power-law at large amplitudes decreases with decreasing temperature. This may reflect that, given that the forward transition goes from a single-domain austenitic crystal to a multidomain martensitic structure, the first martensite domains have more freedom to develop than those formed when approaching the completion of the forward transition. This partitioning effect cuts down the probability of large signals at temperatures close to M_f. This is not observed in the reverse transition since in this case the martensite fraction decreases by the shrinkage of domains, going from a multidomain to a single-domain structure.

C. Correlation function and power spectrum

From the digitized long sequences of AE signals, $\Psi(t)$, we have computed the correlation function $c(t)$ as

$$c(t)=\frac{1}{\Delta}\int_0^{\Delta}\Psi(u)\Psi(t+u)du-\left(\frac{1}{\Delta}\int_0^{\Delta}\Psi(u)du\right)^2 , \quad (3)$$

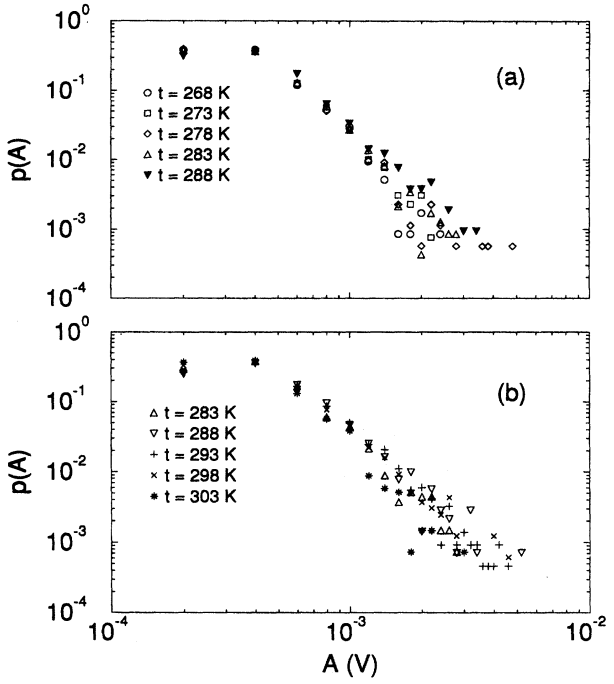

FIG. 5. $p(A)$ at different temperatures for cooling (top) and heating (bottom).

where $\Delta \gg t$ is the total duration of the sequences ($=16$ ms). The inset in Fig. 7 shows the average of $c(t)/c(0)$ over 20 different sequences corresponding to both cooling and heating. Figure 7 shows the corresponding power spectrum

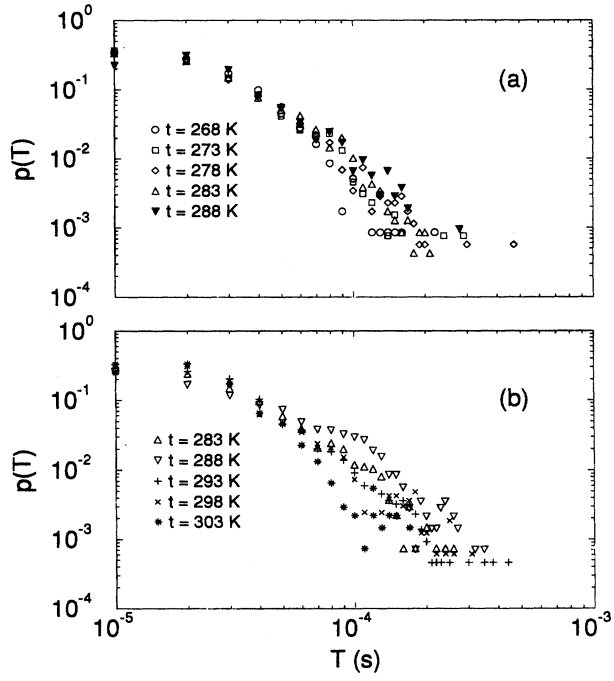

FIG. 6. $p(T)$ at different temperatures for cooling (top) and heating (bottom).

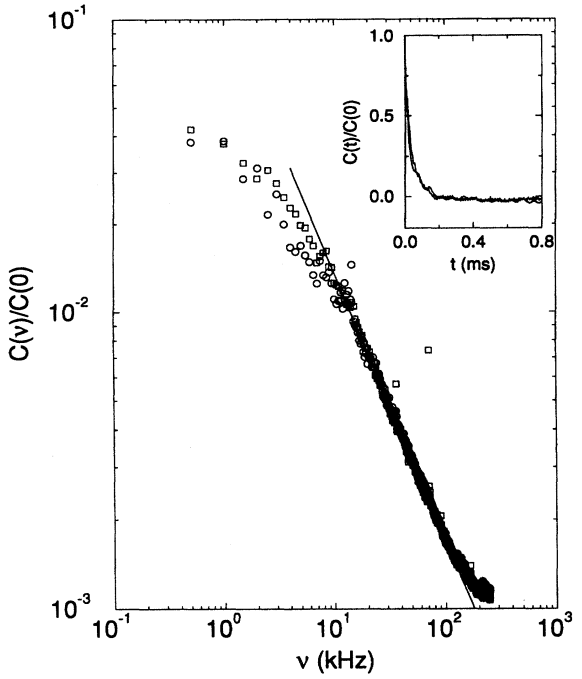

FIG. 7. Power spectrum calculated by Fourier transforming the time correlation functions shown in the inset, for cooling (circles) and heating (squares). The line is a fit in the linear region with slope $\phi=0.9$.

$c(\nu)$ in log-log scales obtained as the numeric Fourier transform of $c(t)/c(0)$, using the fast-Fourier-transform algorithm. We have verified that the peak around 70 kHz originates from the same noise component of the signal discussed in respect to Fig. 2. The curve shows a power-law behavior $c(\nu)\sim\nu^{-\phi}$ in more than one decade. It should be noticed that in this second set of experiments we can scan the high-frequency region more reliably than in the first set due to the fact that we are not using a trigger threshold and, as a consequence, there is no suppression of the short and small signals. In this case, the cutoff at short times is only produced by the sampling frequency of the oscilloscope.

IV. DATA ANALYSIS

The histograms in Figs. 3 and 4 can be fitted to power laws of the form $p(A)\sim A^{-\alpha}$ and $p(T)\sim T^{-\tau}$. For the case of $p(T)$ we have discarded data below 8×10^{-5} s as explained before. We have tried several fitting procedures, leading to slightly different values for the exponents. First, there are two possible ways of building the histograms: (i) using linear bins of width $\Delta V=2\times10^{-4}$ V and $\Delta T=10^{-5}$ s, as in Figs. 3 and 4, and (ii) using logarithmic bins of size 1/10 of a decade. For the two histograms one can perform two kinds of least-squares fitting: (i) a linear regression of $\ln p(X)$ vs $\ln X$ and (ii) a nonlinear fit of $p(X)$ as a power law of X. The results are presented in Table I for $p(A)$ and Table II for $p(T)$, separately for cooling and heating.

The different values arise from the fact that the fitting procedures weight differently the points. If data were exactly distributed according to a power law, all methods would render the same exponents. Actually, the tendency is that values coming from nonlinear fits are smaller than those coming from linear fits. It is not simple to assess which method is more suitable. Since usually, in the literature, fits are performed by a linear regression to linear bins, we will adopt the same criterion to facilitate the comparison with available data; nevertheless, we will consider error bars large enough to include most of the other possibilities. Consequently we take $\alpha=3.8\pm0.8$ and $\tau=3.6\pm0.8$ for cooling, $\alpha=3.5\pm0.8$ and $\tau=3.5\pm0.8$ for heating. Note that the experimental uncertainties do not allow us to establish clear distinctions between cooling and heating values. The value for α found in the present set of experiments is compatible with the value reported previously using a different detection chain.[4] The old detection chain provided very good statistics (a large number of signals could be recorded), but had the inconvenience that the window effect explained in Sec. II was blurred by the complexity of the chain, thus leading to possible misinterpretation of the data. The window effect clearly shows up in the value of τ that we obtain now (when the effect is considered) which considerably differs from the value given in Ref. 4.

TABLE I. Exponents α characterizing the histogram $p(A)$ vs A.

	Linear regression to log-log data		Nonlinear power-law fit	
	Cooling	Heating	Cooling	Heating
Linear bins	3.8	3.5	3.2	2.7
Log. bins	3.9	3.4	3.0	2.6

From the values of α and τ one can calculate the exponent x corresponding to the statistical dependence $A\sim T^x$. For the case of a sharp joint distribution, it has been shown[4] that x is related to α and τ through the following exponent relation:

$$x(\alpha-1)=(\tau-1)\ . \tag{4}$$

Such relation can also be deduced for more general joint distributions using scaling arguments, as will be presented in the following paper (part II). From Eq. (4) one gets $x=0.9$ consistent with the linear behavior of the crest observed in the log-log map of the joint histogram (Fig. 2). An independent method to estimate x is to use the conditional mean value of T for a given A, which should satisfy $\langle T|A\rangle\sim A^{1/x}$.[9] This conditional mean value, computed directly from the recorded signals, is shown in Fig. 8. The results are compatible with the power-law behavior given above. A fit to $\langle T|A\rangle$ (solid line) renders $x=1.0\pm0.1$ for both heating and cooling, in agreement with the value obtained from the scaling relation (4). Finally, the exponent ϕ for the power spectrum $c(\nu)$ has been obtained from a linear

TABLE II. Exponents τ characterizing the histogram $p(T)$ vs T.

	Linear regression to log-log data		Nonlinear power-law fit	
	Cooling	Heating	Cooling	Heating
Linear bins	3.6	3.5	3.9	2.7
Log. bins	4.4	3.7	3.8	2.7

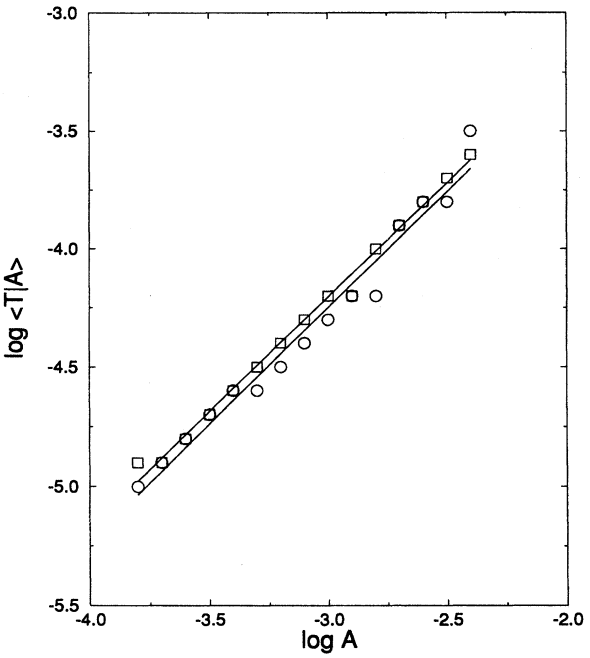

FIG. 8. Conditional mean value $\langle T|A\rangle$ as a function of A for cooling (circles) and heating (squares) in linear scales. The logs are to base 10. The lines are linear fits showing that a power law with exponent $1/x=1$ is compatible with the experimental data.

fit to the power-law region between $\nu=5$ kHz and $\nu=100$ kHz (see Fig. 7). The value obtained is $\phi=0.9\pm0.1$.

V. DISCUSSION

In this work we have characterized the distribution of avalanches in a thermoelastic martensitic transformation by detecting the acoustic emission signals generated. Acoustic emission measurements have also been used to characterize the statistical distribution of avalanches in a number of systems: cracking in volcanic rocks,[10] microfracturing in syntethic plaster,[11] and hydrogen precipitation in niobium.[12] All these systems display power-law behavior for the amplitude distribution of the acoustic events; it is not yet clear, however, that the exponents obtained in such different systems admit a mutual comparison.

The AE technique is particularly suitable for these kind of studies because of its favorable signal-to-noise ratio (which allows us to resolve signals of very different amplitudes) and to its extremely fast response (enabling to discern events with time separations down to μs). Nevertheless, it is worth pointing out some other considerations. First, it is difficult to relate the amplitude and duration of the measured acoustic signals to the physical mechanism giving rise to the acoustic waves. In this respect, it should be stressed that we have used resonant transducers, and therefore the signal duration of a single event could be affected by the damping coefficient of the transducer. Even so, the damping is high for the axial resonant frequencies (the only ones that are not filtered out by the amplifier) and, for this reason, the duration measured for an avalanche (comprising a large number of successive acoustic events) will be comparable to the time elapsed during the avalanche. The time constant for the decay of the axial frequencies is less than the low-duration limit.

Our measurements have shown that thermally induced thermoelastic martensitic transformations take place through avalanches with a wide range of sizes and durations. This behavior seems to be related with the existence of a large amount of disorder in the material: lattice defects such as vacancies, dislocations, and local concentration fluctuations due to off-stoichiometry, quenched-in during the initial thermal treatment of the sample; dislocations created by the martensitic transformation itself[13] along repeated cycling of the crystal; and the heterogeneous elastic strain field arising from the intricate microstructure.[1] This last component of disorder is of a dynamic nature, in the sense that it depends on the domain arrangement and keeps changing during the transformation.

The absence of characteristic scales has been associated with criticality. Recently, there has been a renewed interest in modeling first-order phase transitions in disordered systems by means of reticular models with static random fields or bonds;[5–7] these models show that a critical behavior in the avalanche distributions is associated with a critical amount of disorder. However, the critical region in these models has been shown to be very large,[14] and therefore power-law behavior in a limited number of decades (even for highly sensitive techniques, such as AE) cannot be taken as a definite proof of criticality. In fact, due to the experimental limitations, it is not easy to determine slight deviations from the critical state, either subcritical or supercritical.

Another point to be mentioned is that in models showing disorder-induced first-order phase transitions, at the critical amount of disorder, the power-law exponents depend on the driving field (magnetic field in the models, temperature in our experiments).[5] This is not observed in the experiments presented here: power-law distributions obtained around different temperatures along the transformation path are all characterized by the same exponents. This qualitative difference between models and experiments is still an open question.

To summarize, we have characterized the avalanche distributions in martensitic transformations using AE techniques, and shown to exhibit power-law behavior in more than one decade. We have obtained the exponents for the distributions of amplitudes $\alpha=3.6\pm0.8$ and durations $\tau=3.5\pm0.8$, the exponent characterizing the statistical dependence of amplitude with duration $x=1.0\pm0.1$, and the exponent associated with the power spectrum of the measured signals $\phi=0.9\pm0.1$. Such values are averages between heating and cooling. The measured value of ϕ shows that the behavior of a martensitic transformation is compatible with that of a dynamical system exhibiting $1/f$ noise.

ACKNOWLEDGEMENTS

We acknowledge Jordi Andreu (Universitat de Barcelona) for help in setting up the experimental system. This work has received financial support from the CICyT (Spain), project MAT92-0884.

[1] A. G. Khachaturyan, *Theory of Structural Transformations in Solids* (Wiley, New York, 1983); M. Cohen, G. B. Olson, and P. C. Clapp, *Proceedings of the International Conference on Martensitic Transformations* (Cambridge, MA, 1979), pp. 1–11.

[2] A. A. Pollock, Int. Adv. Nondestr. Test. **7**, 215 (1981).

[3] Ll. Mañosa, A. Planes, D. Rouby, M. Morin, P. Fleischmann, and J. L. Macqueron, Appl. Phys. Lett. **54**, 2574 (1989); Ll. Mañosa, A. Planes, D. Rouby, J. L. Macqueron, Acta Metall. Mater. **38**, 1635 (1990).

[4] E. Vives, J. Ortín , Ll. Mañosa, I. Ràfols, R. Pérez-Magrané, and A. Planes, Phys. Rev. Lett. **72**, 1694 (1994).

[5] J. P. Sethna, K. Dahmen, S. Kartha, J. A. Krumhansl, W. Roberts, and J. D. Shore, Phys. Rev. Lett. **70**, 3347 (1993); K. Dahmen and J. P. Sethna, *ibid.* **17**, 3222 (1993); J. P. Sethna, K. Dahmen, S. Kartha, J. A. Krumhansl, O. Perkovic, B. W. Roberts, and J. D. Shore, *ibid.* **72**, 947 (1994).

[6] E. Vives and A. Planes, Phys. Rev. B **50**, 3839 (1994).

[7] J. Goicoechea and J. Ortín, J. Phys. IV (France) **5**, 71 (1995).

[8] A recorded signal begins when, on rising, crosses the three threshold levels in ascending order and ends when, on falling, crosses again the three threshold levels in descending order. The duration is given by the time interval between the two crossings of the middle threshold.

[9] The relation can be easily derived from dimensional arguments. A rigorous demonstration is given in paper II.

[10] P. Diodati, F. Marchesoni, and S. Piazza, Phys. Rev. Lett. **67**, 2239 (1991).

[11] A. Petri, G. Paparo, A. Vespignani, A. Alippi, and M. Constantini, Phys. Rev. Lett. **73**, 3423 (1994).

[12] G. Cannelli, R. Cantelli, and F. Cordero, Phys. Rev. Lett. **70**, 3923 (1993).

[13] F. C. Lovey, A. Amengual, and V. Torra, Philos. Mag. A **64**, 787 (1991).

[14] K. Dahmen, O. Perkovic, and J. P. Sethna (unpublished).